JOURNAL OF MATERIALS SCIENCE 26 (1991) 2081–2088

Interfacial factors affecting the incidence of defects in ceramic mouldings

J. R. G. EVANS, M. J. EDIRISINGHE
Department of Materials Technology, Brunel University, Uxbridge, Middlesex, UB8 3PH, UK

Ceramic injection moulding suspensions consisting of two alumina powders of surface area 9.5 $m^2 g^{-1}$ and 0.3 $m^2 g^{-1}$ were prepared at 60 vol% ceramic loading in the same organic composition. Cylinders of various diameters of each suspension were companion fired on an identical temperature ramp in nitrogen. For the fine powder, bloating occurred for all diameters above 8 mm. The coarse powder cylinders of 25 mm diameter could be prepared free from internal voids. The problems presented by fine powders during binder removal are discussed in terms of adsorbed layers, water emission and catalytic degradation.

1. Introduction

The fabrication of complex shapes by injection moulding is used increasingly for small section components (< 15 mm) and the problems of preparing large components continue to be explored [1, 2]. It is generally recognized that removal of the organic vehicle places restrictions on section size but there is, as yet, little quantitative study of the mass transport kinetics which control the exodus of organic vehicle or its degradation products.

In principle, the injection moulding operation should be capable of serving the entire range of ceramic powders. Particle size distribution (PSD) influences the volume fraction of ceramic that can be incorporated in suspension [3] just as it influences the packing of particles in pressing or casting operations. Fine powders tend to sustain a lower volume loading [4] and this can be attributed to the influence of adsorbed polymer layers on effective volume fraction [5]. An observation of some concern is, that the removal of organic vehicle from moulded ceramic bodies was facilitated when coarse ceramic powders were used [6]. Modern developments in ceramic powders favour uniform unagglomerated fine particles [7]. The reason for these developments are: (i) the increase in the driving force for sintering; (ii) the reduction of diffusion distances on sintering and (iii) the minimization of the driving force for grain growth. It therefore becomes necessary to establish the effects of particle size on binder removal by controlled experiments before commencing the difficult task of quantifying the binder removal transport processes.

In the injection moulded ceramic body, organic vehicle fills the entire pore space [3] unlike the binder used in pressing operations which fills only a fraction of the pore space. Removal of the binder by pyrolysis can take place by three mechanisms [8, 9]: (i) oxidation at the surface followed by evaporation of oxidative degradation products; (ii) diffusion and evaporation of low molecular weight species already present in the binder; (iii) thermal degradation of the binder followed by diffusion in the bulk and evaporation of degradation products which are lower than a critical size.

On heating a large moulded body, thermal degradation takes place to some extent throughout the body and generates low molecular weight species which can only be lost by evaporation from the surface. The combination of decomposition and evaporation sets up a concentration profile throughout the body which provides a driving force for diffusion of products in solution through the ceramic–polymer suspension towards the surface [10]. If the centre concentration rises above a critical level at a given temperature and pressure, boiling ensues and voids are formed [10].

In the present work two alumina powders of widely differing mean particle size and specific surface area were selected and suspensions of each were prepared at the same volume loading in the same organic vehicle. The defects resulting from binder removal from identical cylinders prepared from each powder were compared.

2. Experimental procedure

A16 SG alumina with a specific surface area (SSA) of 9.5 $m^2 g^{-1}$ was obtained from Alcoa GB Ltd. MA2LS alumina with a SSA of 0.22 $m^2 g^{-1}$ derived from PSD or 0.30 $m^2 g^{-1}$ quoted by the manufacturer was donated by Alcan Chemicals Ltd. Fig. 1 shows the particle size distributions. The organic vehicle consisted of isotactic polypropylene, atactic polypropylene and stearic acid in the weight ratio 4:4:1. Atactic polypropylene was grade MF5 from APP Chemicals of Salop UK and isotactic polypropylene was grade GY545M from ICI.

Mixing was carried out using the procedure previously described for composition F11 [11]. Premixing was carried out in a Henschel high speed mixer and dispersive mixing was achieved by a Betol TS40 twin screw extruder using barrel temperatures (feed to exit) 190–195–210–205 °C. The compositions are

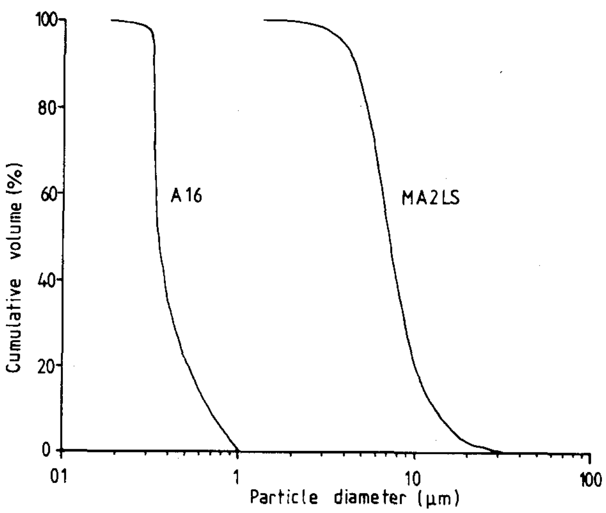

Figure 1 Particle size distributions for the two alumina powders.

TABLE I Compositions of ceramic suspensions

	Weight per cent 1	 2
Alumina A16SG	87.27	–
Alumina MA2LS	–	87.36
Atactic polypropylene	5.66	5.62
Isotactic polypropylene	5.66	5.62
Stearic acid	1.41	1.40
Alumina (volume %)	60.6	60.7

shown in Table I which includes the ceramic volume loading calculated from the mean of four ashing experiments.

Iron analysis on the powders after twin screw extrusion was performed by Leeds Mining Consultants Ltd. (Kirkstall, Leeds, UK). Molecular weight distribution by GPC was carried out by RAPRA (Shrewsbury, UK).

Compression moulded cylinders of diameter 8, 18, 25 and 31 mm were prepared in an Apex model M1/R press at 190 °C under 12 MPa pressure. These were radiographed after manufacture using a Hewlett Packard Faxitron contact radiography camera. Compression moulding was used in preference to injection moulding for simplicity of fabrication of a small number of different size components.

The cylinders were heated in flowing oxygen-free nitrogen at 60 °C h^{-1} to 150 °C and held for 24 h. The temperature was then increased at 2 °C h^{-1} to 350 °C, held for 24 h and again increased at 2 °C h^{-1} to 450 °C before furnace cooling. During this process, pairs of samples of identical dimension, but of each alumina, were companion-fired. The resulting internal structure was revealed by X-ray radiography immediately after polymer removal and the cylinders were partially sintered. Partial sintering was effected at 1200 °C for 30 min for A16 and at 1500 °C for 30 min for MA2LS in order to confer sufficient strength for subsequent handling.

A Stanton TR1 thermobalance was used for thermogravimetry of samples of the suspension which had been granulated to pass a 710 µm sieve. Samples of the as-received powders were heated in the thermobalance to obtain the water desorption characteristics.

3. Results and discussion

3.1. Defects in mouldings

Fig. 2 shows prints of the X-ray radiographs of compression moulded cylinders after manufacture indicating that they are free from macroscopic defects. Fig. 3 shows prints of the X-ray radiographs of cylinders of both powders after removal of the organic vehicle. Using the temperature ramp described, the maximum radius of cylinder of those studied, that could be manufactured with the polypropylene based organic vehicle without internal defects was 8 mm for the fine A16 powder. For the coarse MA2LS powder, cylinders of 25 mm could be produced without internal defects and cylinders of 31 mm could be prepared with a small void nucleated at the centre exactly in the position expected from consideration of the concentration profile of degradation products.

Of considerable interest is the array of defects seen in Fig. 4. This shows a 25 mm diameter cylinder of MA2LS which had been supported in the furnace on a crucible machined from an alumina furnace tube. By coincidence, the internal diameter of the tube on which this sample rested, was similar to the cylinder diameter. The ceramic body had, during polymer removal, made good contact with the crucible and diffusion through this region of the surface was impeded. The arc over which defects are seen in Fig. 4 corresponded to the position of the crucible at the surface. In similar samples supported freely these defects were not present (Fig. 3). Fig. 5 shows the bloating observed in the A16 alumina samples. It is noteworthy that the bloating has occurred at a stage where the suspension behaved as a fluid, that is to say in the early stages of removal before the suspension acquired *quasi*-solid properties as a result of loss of organic phase.

The removal of polypropylene by thermal degradation in an inert atmosphere involves chain scission, diffusion of molecular fragments to the surface followed by evaporation and it is therefore expected that the sample diameter will exert a pronounced effect on the concentration of degradation products in solution in the polymer and hence on the incidence of defects.

It seems likely that for a given organic vehicle and a given thermal schedule there will be a maximum diameter from which organic removal can occur without defects. What is very surprising is the striking dependence of this critical diameter on particle characteristics for these two aluminas. The following causes can be hypothesized for this effect:

(i) The impediment to diffusion in the melt imposed by adsorbed polymer layers.
(ii) The release of adsorbed water.
(iii) The catalytic effect of the alumina on polymer degradation.

These causes will now be discussed.

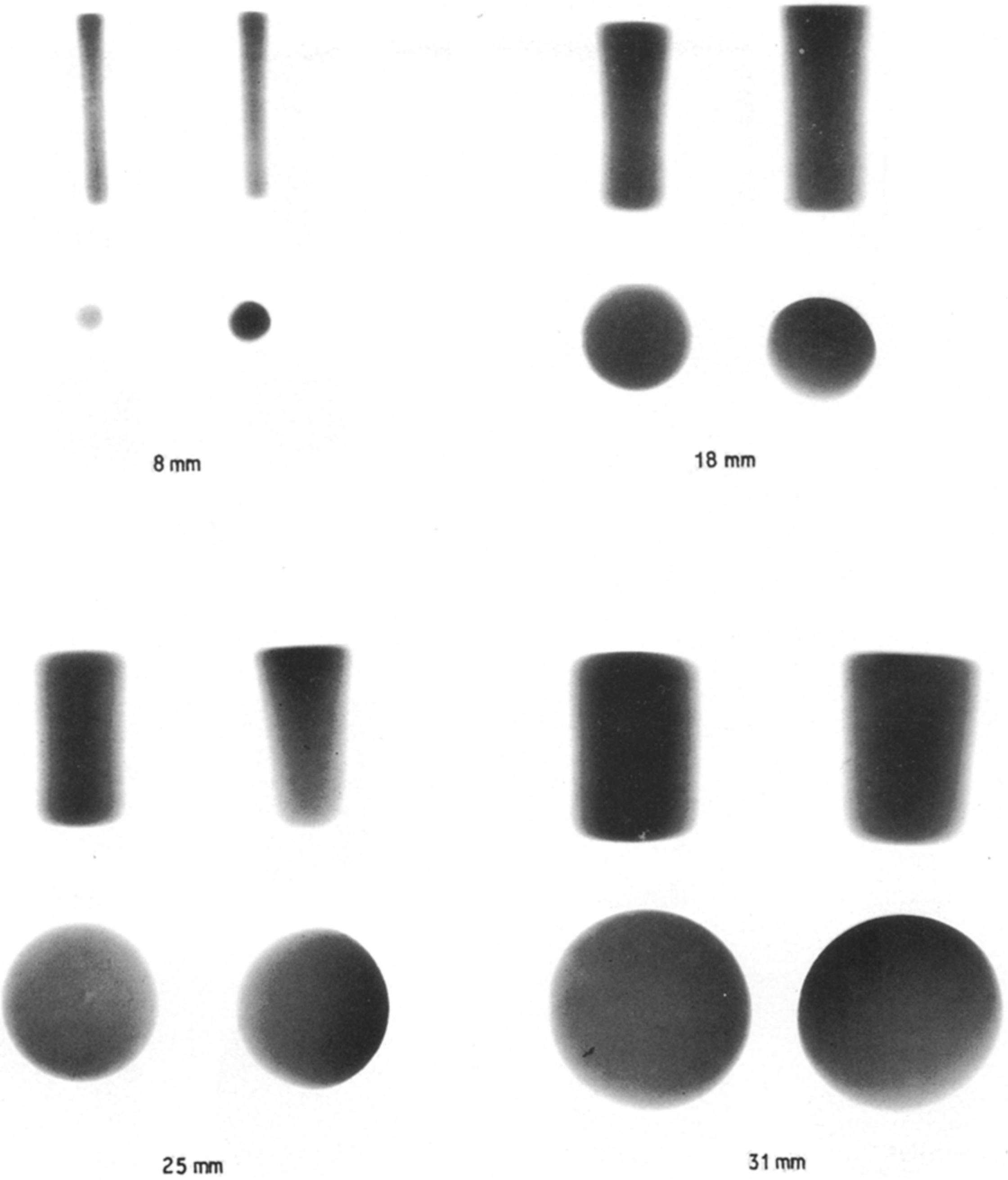

Figure 2 Prints of X-ray radiographs of cylinders before heat treatment. For each pair, the coarse powder is on the left, the fine powder on the right.

3.2. Effect of adsorbed polymer layers

Diffusion in two phase media has been reviewed by Barrer [12] who, relying on the similarity of expressions for electrical and mass transport processes, presents equations relating diffusion coefficient in a particle filled suspension D to diffusion coefficient in the continuous phase D_2 for a volume fraction of dispersed phase V_1. For the case where diffusion in the dispersed phase is negligible, these are:

(i) Maxwell model

$$\frac{D}{D_2} = 1 - \frac{3V_1}{V_1 + 2} \tag{1}$$

for $V_1 = 0.6$, $D/D_2 = 0.31$

(ii) Rayleigh model

$$\frac{D}{D_2} = \frac{2 - 2V_1 + 1.238\ V_1^{10/3}}{2 + V_1 + 1.238\ V_1^{10/3}} \tag{2}$$

for $V_1 = 0.6$, $D/D_2 = 0.36$

(iii) Bruggerman model

$$\frac{D}{D_2} = (1 - V_1)^{3/2} \tag{3}$$

for $V_1 = 0.6$, $D/D_2 = 0.25$

More recently, Bedeaux and Kapral [13] and Sridharan and Cukier [14] present models which

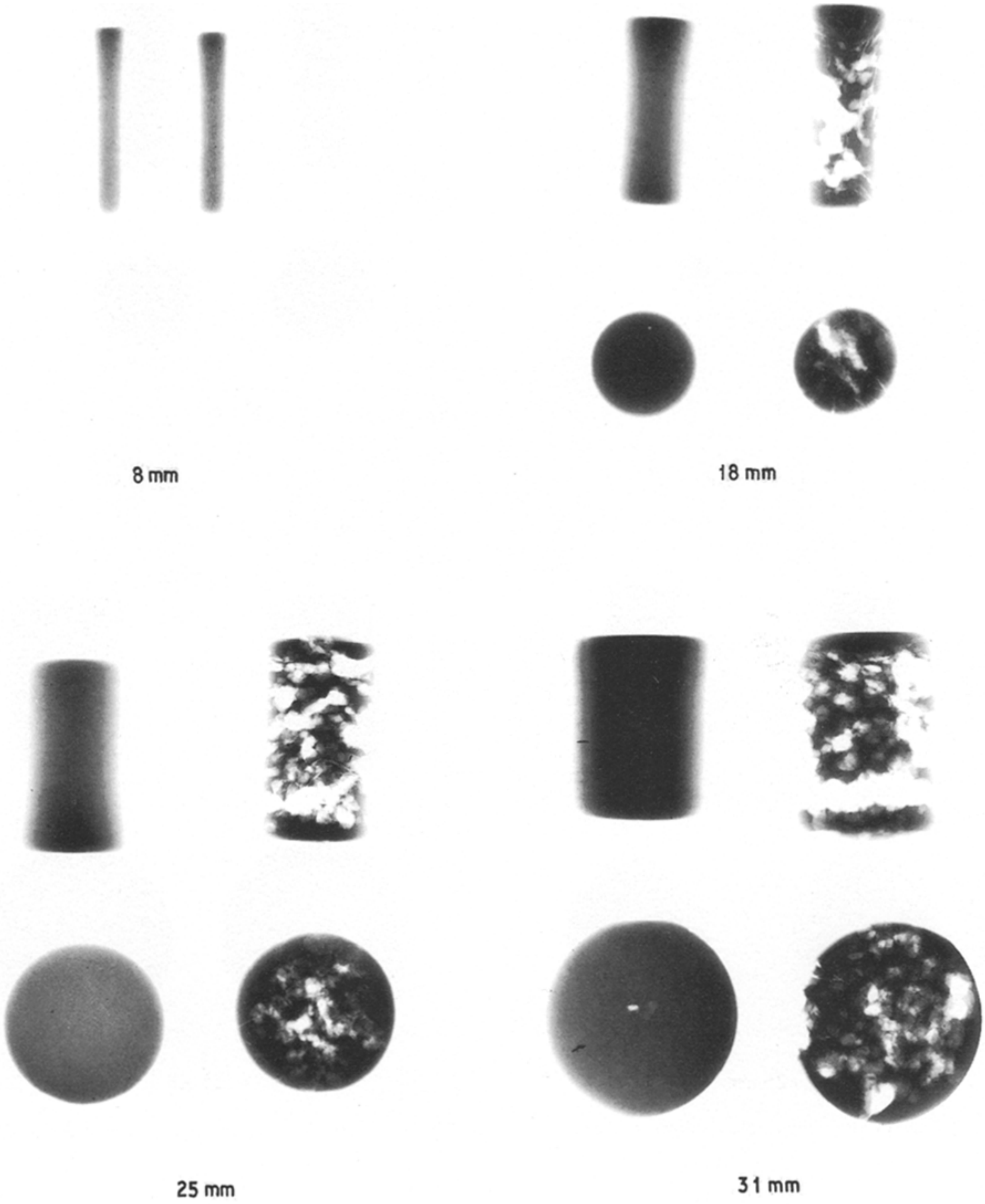

8 mm

18 mm

25 mm

31 mm

Figure 3 Prints of X-ray radiographs of cylinders after heat treatment. For each pair, the coarse powder is on the left, the fine powder on the right.

reduce, for zero diffusion in the dispersed phase to

$$\frac{D}{D_2} = 1 - 1.5V_1 \qquad (4)$$

$$\text{for } V_1 = 0.6, \quad D/D_2 = 0.1$$

This equation has the unfortunate limitation that diffusivity in the composite is predicted to be zero at $V_1 = 0.67$.

Experimental validation of these models for diffusion at high volume fractions is understandably sparse but is necessary for the quantitative analysis of the removal of organic vehicle. Of considerable concern, however, is the fact that these models consider only volume fraction of dispersed phase and neglect the influence of particle characteristics on D/D_2.

It is not reasonable to suppose that the entire interstitial space is available for unimpeded diffusion in the polymer melt. Adsorption of polymer or wax molecules on the ceramic walls of the pore may create an immobile layer. In filled polymers such layers can extend up to 150 nm from the high energy surface of minerals [15]. Within this region polymer segment mobility is restricted.

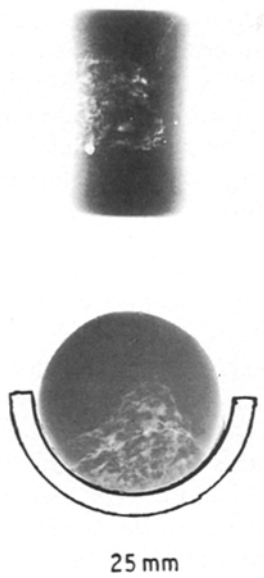

Figure 4 Prints of an X-ray radiograph of a coarse alumina powder sample showing the impediment to diffusion afforded by the crucible.

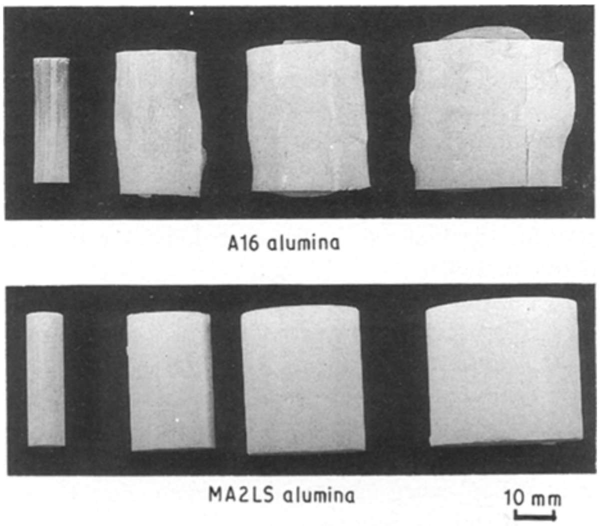

Figure 5 Visual appearance of the cylinders after binder removal and partial sintering.

Polymer adsorption involves short sequences which are attached to the surface separated by loops which extend well into the matrix [16]. These influence the dynamic mechanical spectra for filled polymers where a striking effect of mineral surface area is observed [17]. They influence the glass transition temperature of solid polymers [18] and the viscosity of suspensions [19]. Most attempts to measure the dimensions of adsorbed layers use polymer solutions. A study of the adsorption of polystyrene on glass, performed by following the build up of an adsorbed layer from solution on a glass capillary viscometer showed that the hydrodynamic layer thickness was comparable to the dimensions of a random coil for the polymer adsorbate and was in the region 5–100 nm for the range of molecular weights employed [20]. Comparable adsorption layers were obtained for polystyrene on chromium [21]. Other experiments have measured the increase in resistance to flow of polymer solutions through sintered glass discs caused by adsorption and related adsorbed layer thickness to the dimensions of a random coil [22]. Restrictions on segment mobility sufficient to have these effects, are also likely to have an influence on the diffusion coefficient for small molecules migrating in the melt. For a random coil, the end to end distance (h) characterizes the dimensions of the molecule in solution and is given by [23]

$$h^2 = n\,l^2 \frac{(1 - \cos\theta)}{(1 + \cos\theta)} \tag{5}$$

where n is the number of links in the molecule, l is the bond length and θ is the bond angle. For polyolefins $\theta = 109.5°$, hence $h^2 \approx 2nl^2$. However additional restrictions on chain mobility increase the effective bond length and Equation 5 can be expressed as

$$h^2 = n\beta^2 \tag{6}$$

where β is determined experimentally. In general $\beta \approx 3l$ [23]. The coil dimensions in the melt are expected to be similar to those in solution and Table II shows calculated random coil dimensions for polymers and waxes used in previous ceramic injection moulding studies [11, 24].

It is of considerable interest to compare these dimensions with those of the pore architecture in a prefired ceramic body. The smallest hole in the pore structure of close packed uniform sized ceramic spheres of radius r is the inscribed circle between three contacting particles and the radius of that circle is $0.155r$ [25]. Table III shows the order of magnitude of this pore size for a range of ceramic powders. The exact pore size cannot be determined because the

TABLE II Calculated random coil dimensions for polymers used in ceramic injection moulding

Polymer	Molecular weight (M_n)	Average end to end distance (nm)
Microcrystalline wax (Astor Chemical, UK)	300	3
Atactic polypropylene (APP Chemicals, UK)	2900	5
Low density polyethylene (BP Chemicals, UK)	12500	14
Polypropylene (ICI plc)	31850	18
Polystyrene (BP Chemicals, UK)	101400	20

TABLE III Estimate of pore radius for a range of commercial powders

Ceramic Powder	Average particle diametre (μm)	Pore radius (nm)
Alumina MA2LS (Alcan)	6	460
Alumina A16SG (Alcoa)	0.4	30
Zirconia HSY3 (Daiichi-kigenso)	0.2	15
Zirconia Dynazircon F (Dynamit Nobel)	0.1[a]	8

[a] By scanning electron microscopy.

powders are neither monodisperse nor spherical. Neither does the condition of perfect close packing apply to these commercial powders in most fabrication processes, but the illustration serves to show that the removal of organic binders may require molecules to move through very small channels. Indeed a wide particle size distribution leading to more efficient ceramic packing may result in smaller pore channels [25]. The space which is available as a diffusion path is expected to be reduced by a function of the thickness of the adsorbed layer.

Comparison of the estimated distances in Tables II and III suggest that where a high polymer is combined with a fine ceramic, an adsorbed layer may actually fill the available pore space and coefficients of diffusion for small molecules migrating in the polymer melt could be substantially reduced below the values measured for bulk systems, a factor unaccounted for by Equations 1–4. At present, measured values of diffusivity for systems involving ceramic powders are not available.

It is proposed that as an initial step in accommodating the influence of particle characteristics on diffusion, the term D/D_2 should be redefined

$$D/D_2 \;=\; f(V_1, \mathrm{S}, h) \qquad (7)$$

where S is the specific surface area of the ceramic powder and h is the chain end to end distance for the polymer or wax. Several expressions for D/D_2 as a function of volume fraction of ceramic were given in Equations 1–4 and these require validation by experiments with coarse powders where adsorption effects are negligible. The effective volume fraction of ceramic can then be redefined for fine powders as

$$V \;=\; V_1\,(1 + \mathrm{k}\rho_\mathrm{c}\mathrm{S}h) \qquad (8)$$

where ρ_c is the ceramic density ($3987\,\mathrm{kg\,m^{-3}}$). k is a constant ($0 \leq \mathrm{k} \leq 1$) which defines the effective thickness of the adsorbed layer for which diffusivity is zero. The dimensionless term on the right-hand-side is thus the effective increase in volume fraction of ceramic caused by adsorbed layers. Putting $\mathrm{k} = 1$ assumes that diffusion in the entire adsorbed phase is zero. Substituting values for the two types of alumina and for the isotactic polypropylene and putting $\mathrm{k} = 0.5$, the effective volume fractions in the above experiment where $V = 81$ vol % for A16 alumina with a specific surface area of $9500\,\mathrm{m^2\,kg^{-1}}$ and 61.2 vol % for the MA2LS alumina with a specific area of $220\,\mathrm{m^2\,kg^{-1}}$. Substituting the value for A16 alumina in Equation 1 gives $D/D_2 = 0.14$ compared with 0.30 for MA2LS. The situation becomes more serious during shrinkage as polymer is removed. Previous work has shown that A16 alumina moulded at 60 vol % continued to shrink as organic vehicle was removed until the effective volume fraction rose to 65 vol % [26]. The effective volume loading calculated from Equation 8 is then 87 vol %, giving $D/D_2 = 0.09$. This is the point of minimum diffusion because thereafter pores are obliged to form; further shrinkage being impeded by particle contact.

Ceramic injection moulding suspensions cannot, however, be treated as pure polymer–ceramic systems. Low molecular weight additives are normally included as lubricants or plasticizers [3]. A favoured additive is a carboxylic acid [11, 24] and coupling agents have also been employed [27]. These species may be capable of strong adsorption on ceramic surfaces and may act either by occupying adsorption sites and displacing polymer molecules or by enhancing polymer adsorption by the formation of an interpenetrating network [28].

3.3. Exodus of adsorbed water

The presence of adsorbed water layers on high energy surfaces is well-known [29] and adsorption forces are sufficiently strong that ceramic surfaces are not freed from water until high temperatures or very low pressures. Fig. 6 shows thermogravimetric traces for the loss of water from the A16 alumina powder. An identical experiment on the MA2LS powder showed no weight loss. A sample of A16 alumina was retested after equilibration in ambient air for 48 h and showed a lower weight loss. Although some reduction in surface area may result from heating the powder to 500 °C it is likely that organic matter was responsible for the loss at temperatures above about 200 °C. Since the maximum processing temperature was 210 °C the bulk of the water is expected to be displaced during mixing and only 0.04 wt % based on the alumina remains to be discharged from the surface in the temperature range 210–400 °C. This reasoning rests on two assumptions: (a) that the compounding process prevents subsequent water adsorption and (b) that the curve for the first run in Fig. 6 includes the loss of organic matter.

With a low molecular weight organic vehicle such as a wax, processed at lower temperatures, more water would await discharge during the pyrolysis stage. It is easy to show that the adsorbed water which is liberated between 200 and 400 °C in the A16 alumina cylinders represents 2.7 times the volume of the cylinder at 400 °C when converted to steam. For a wax based suspension processed at 100 °C this volume ratio would be 19. The water must be regarded as an unwelcome constituent of the organic vehicle which

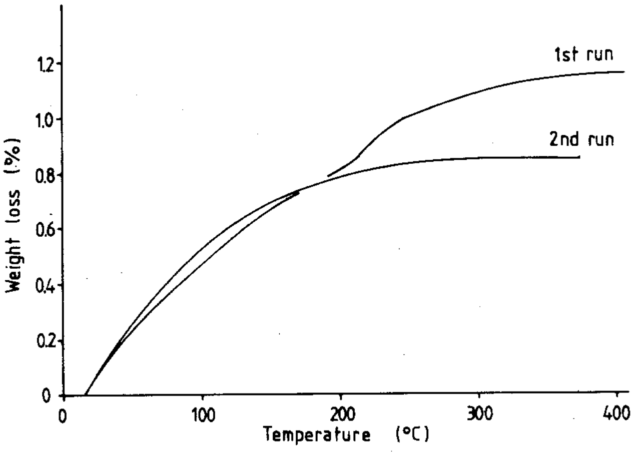

Figure 6 Thermogravimetric loss from the A16 alumina powder at 2 °C min^{-1} in air.

must be removed by diffusion in the melt. An interesting feature of this problem is that the large displaced volume of water arises from the low molecular weight of water while on the other hand the small molecular size of the water molecule aids diffusion.

Values for the water permeability of polymers make clear that permeability is strongly influenced by polymer polarity [30] and therefore polyolefins either as waxes or high polymers have a disadvantage in that the diffusion of water is low. It is, however, likely to be influenced by the extent of oxidation of the polyolefin brought about during mixing and pyrolysis. Long mixing schedules are known to cause extensive oxidation [31], but in the present work oxidation was minimized by twin screw extrusion [32] and pyrolysis was carried out in an inert atmosphere. Interruption of the ramp at 250 °C for 25 mm cylinders of A16 showed that bloating had occurred by that temperature.

These observations offer an alternative but not unrelated explanation for the distinct behaviour of the two powders. It is generally observed that the presence of adsorbed layers on fillers also reduces the water permeability of polymers [15] so that high surface area powders present combined problems for ceramic injection moulding which must be addressed by careful selection of organic species. In the present example however, the use of high processing temperatures has removed most adsorbed water and this is not considered to be the main cause of the defects in Fig. 3.

3.4. Catalysis of degradation processes

It is well known that transition metals catalyse the oxidation of polymers [33] but a wide range of ceramic powders have been shown to catalyse both the oxidation and thermal degradation of polyvinyl butyral [34]. Since the extent of such catalysis is expected to depend, *inter-alia*, on powder surface area, the thermogravimetric weight loss of both alumina–polypropylene samples was measured. Although Fig. 7 shows a slight difference between the curves, it has been noted that there is a poor correlation between the form of the thermal gravimetric analysis (TGA) curve and the incidence of defects for ceramic suspensions based on polypropylene [8]. In fact the difference may not have resulted from the catalytic influence of the powder during pyrolysis but from the different extents of mechanical degradation during extrusion. Some evidence for this is obtained from the polymer molecular weight distributions obtained on samples immediately after twin screw extrusion, which are shown in Fig. 8. The increase in the low molecular weight fraction of polypropylene in blend 2 probably accounts for the deviation in the TGA curve (Fig. 7) and results from the mixing operation. Thus no noticeable catalytic effect of the difference in specific surface areas of the aluminas is obtained.

The iron analysis based on the weight of alumina after ashing reveals the different mixing behaviour of the two powders. The A16SG alumina contained 100 p.p.m. Fe while the MA2LS alumina contained 330 p.p.m. Fe. The MA2LS composition after extrusion was visibly grey. The catalysis of the oxidative degradation of polypropylene by iron during binder removal does not occur because the pyrolysis was performed in an inert atmosphere.

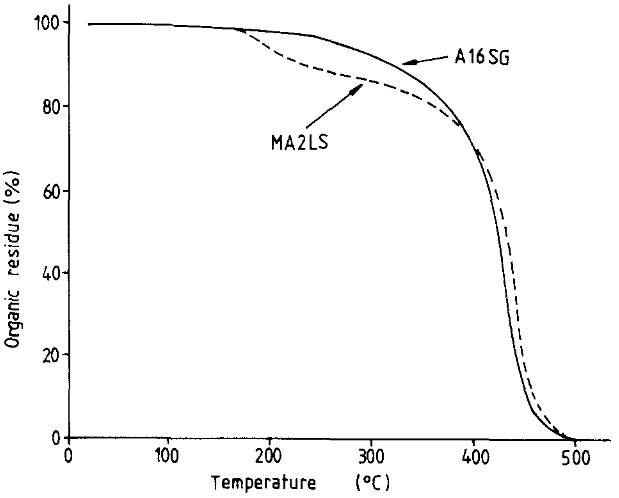

Figure 7 Thermogravimetric loss of both moulding blends in flowing nitrogen at 2 °C min^{-1}.

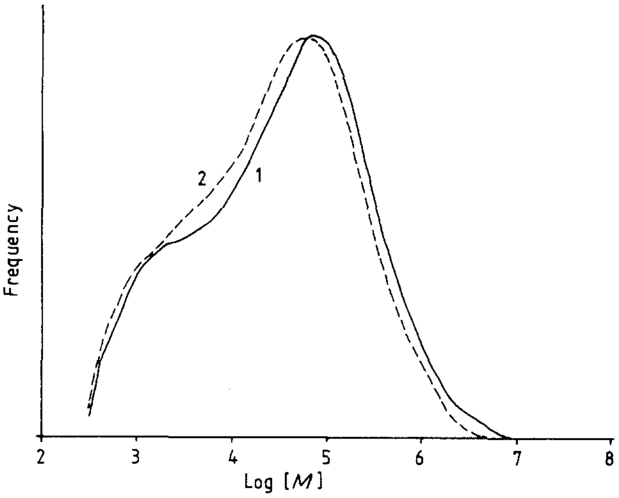

Figure 8 Polypropylene molecular weight distributions for compositions 1 and 2 after extrusion.

4. Conclusions

Ceramic moulding compositions prepared with the same organic vehicle at the same volume loading of pure alumina powder of widely different surface area show markedly different behaviour during pyrolysis of the organic vehicle in oxygen-free nitrogen. The maximum diameter of cylinder that can be pyrolysed without the incidence of defects was 8 mm for a 9500 $m^2 g^{-1}$ powder and 25 mm for a 220 $m^2 g^{-1}$ powder. Several causes can be advanced for the effect of powder characteristics

(i) The obstruction of diffusion in the polymer melt within the interstitial pore space caused by immobile adsorbed polymer layers.

(ii) The emission of adsorbed water from high surface area powders which in turn is obstructed by adsorbed polymer layers.

(iii) The catalytic effect of the powder on thermal degradation of the polymer.

(iv) The slight difference in molecular weight distribution caused by processing different powders in high shear.

Of these the first is regarded as the most likely cause and much further work is needed to quantify the mass transport of degradation products in ceramic suspensions.

Acknowledgements

The authors are grateful to SERC for supporting the ceramic fabrication programme.

References

1. J. G. ZHANG, M. J. EDIRISINGHE and J. R. G. EVANS, *J. Euro. Ceram. Soc.* **5** (1989) 63.
2. *Idem., J. Mater. Sci.* **24** (1989) 840.
3. M. J. EDIRISINGHE and J. R. G. EVANS, *Int. J. High Tech. Ceram.* **2** (1986) 1.
4. K. M. HUNT, J. R. G. EVANS and J. WOODTHORPE, *Brit. Ceram. Trans. J.* **87** (1988) 17.
5. A. DOROSZKOWSKI and R. LAMBOURNE, *J. Coll. Interf. Sci.* **26** (1968) 214.
6. M. J. EDIRISINGHE, *Proc. Brit. Ceram. Soc.* **45** (1990) 109.
7. E. A. BARRINGER and H. K. BOWEN, *J. Amer. Ceram. Soc.* **65** (1982) C199.
8. J. WOODTHORPE, M. J. EDIRISINGHE and J. R. G. EVANS, *J. Mater. Sci.* **24** (1989) 1038.
9. J. K. WRIGHT, J. R. G. EVANS and M. J. EDIRISINGHE, *J. Amer. Ceram. Soc.* **72** (1989) 1822.
10. J. R. G. EVANS, M. J. EDIRISINGHE, J. K. WRIGHT and J. CRANK, *Proc. Roy. Soc. A*, in press.
11. M. J. EDIRISINGHE and J. R. G. EVANS, *Brit. Ceram. Trans. J.* **86** (1987) 18.
12. R. M. BARRER, in "Diffusion in Polymers", edited by J. Crank and G. S. Park (Academic Press, London, 1968) p. 165.
13. D. BEDEAUX and R. KAPRAL, *J. Chem. Phys.* **79** (1983) 1783.
14. S. SRIDHARAN and R. I. CUKIER, *J. Phys. Chem.* **91** (1987) 2962.
15. T. K. KWEI, *J. Polym. Sci.* **A3** (1965) 3229.
16. R. R. STROMBERG, in "Treatise on Adhesion and Adhesives", Vol. 1, edited by R. L. Patrick (Dekker, N.Y., 1967) pp. 69–118.
17. J. JANCAR, J. KUCERA and P. VESSELY, *J. Mater. Sci. Lett.* **7** (1988) 1377.
18. K. IISAKA and K. SHIBAYAMA, *J. Appl. Polym. Sci.* **22** (1978) 1321.
19. T. SATO, *J. Appl. Polym. Sci.* **15** (1971) 1053.
20. Z. PRIEL and A. SILBERBERG, *J. Polym. Sci. A2 Polym. Phys.* **16** (1978) 1917.
21. M. KAWAGUCHI and A. TAKASHASHI, *ibid.* **18** (1980) 2069.
22. F. W. RYLAND and F. R. EIRICH, *J. Polym. Sci. A1*, **4** (1966) 2401.
23. C. TANFORD, in "Physical Chemistry of Macromolecules" (Wiley, N.Y., 1967) pp. 150–161.
24. M. J. EDIRISINGHE and J. R. G. EVANS, *J. Mater. Sci.* **22** (1987) 269.
25. D. J. CUMBERLAND and R. J. CRAWFORD, in "The Packing of Particles" (Elsevier, Amsterdam, 1987) p. 60.
26. J. K. WRIGHT, M. J. EDIRISINGHE, J. G. ZHANG and J. R. G. EVANS, *J. Amer. Ceram. Soc.* **73** (1990) 2653.
27. J. G. ZHANG, M. J. EDIRISINGHE and J. R. G. EVANS, *J. Mater. Sci.* **23** (1986) 2195–2120.
28. E. P. PLUEDDEMAN and G. L. STARK, in Proceedings of the 35th Annual Tech. Conference Soc. Plast. Eng. (1980) 20B-1.
29. M. K. BERNETT and W. A. ZISMAN, *J. Coll. Interf. Sci.* **28** (1968) 243.
30. C. E. ROGERS, in "Physics and Chemistry of the Organic Solid State", edited by D. Fox, M. M. Labes, A. Weinberger (Interscience, N.Y., 1965) p. 509.
31. K. N. HUNT, J. R. G. EVANS and J. WOODTHORPE, *Brit. Ceram. Trans. J.* **87** (1988) 17.
32. J. ABRAM, J. BOWMAN, J. C. BEHIRI and W. BONFIELD, *Plast. Rubb. Proc. Appl.* **4** (1984) 165.
33. S. A. CHAUDRI, *Polymer* **9** (1968) 604.
34. S. MASIA, P. D. CALVERT, W. E. RHINE and H. K. BOWEN, *J. Mater. Sci.* **24** (1989) 1907.

Received 29 November 1989
and accepted 20 April 1990